CHAPTER 2

Literature Review

2.1 Zeolites

Zeolites are a family of hydrated aluminosilicate minerals that contain alkali and alkaline-earth metals [2]. Consisting of interlocking tetrahedrons of SiO_4 and AlO_4 that extend infinitely, they are characterized by a three-dimensional tetrahedral framework in which each oxygen atom is shared by two tetrahedra (Fig. 2.1). Different types of zeolites are differentiated by the number of sodalite cages and the way they are arranged. They can be pictured as large frameworks consisting of pores interconnected by channel windows. The ideal formula for a zeolite stated by Smith [3] is given as:

$$M_pD_q[Al_{p+2q}Si_rO_{2p+4q+2r}] \cdot sH_2O$$

M = monovalent ions

D = divalent ions

Smith [3] also noted that in order for the zeolite structure to remain neutral the number of trivalent aluminum ions has to equal the total number of monovalent ions (p) and twice the number of divalent ions (q). This is due to the presence of aluminum in the aluminosilicate framework which creates a charge imbalance, requiring the presence of other metal cations in the cavities. The other variables r and s are independent integers.

Natural zeolites occur in cavities of volcanic rock, a result of very low-grade metamorphism. From a research standpoint, synthetic zeolites provide a consistent grade of purity compared with natural zeolites, which are generally contaminated with clays, quartz, feldspars, and volcanic glass, up to the extent of 20% [4].

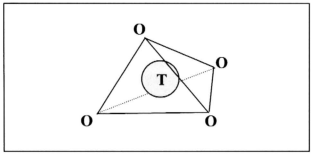

Fig. 2.1: A schematic representation of the tetrahedra of which zeolites are made up. T is either Si or Al. The tetrahedra join by sharing O at the corners and extend in three-dimensions infinitely to make up the aluminosilicate framework.

The zeolites used in this study are of the synthetic Y type, containing sodium cations, thus it is named Na-Y zeolite. Its chemical formula is $Na_{56}Al_{56}Si_{136}O_{384}{\bullet}250H_2O$. A schematic of a zeolite Y molecule is shown in Fig. 2.2. This structure is in the dehydrated state because excess water is always present after synthesis and is easily driven off by heating. Water molecules present in hydrated systems stick to and surround the metal ions which then occupy ill-defined sites in the voids and channels [5]. These loosely bound hydrated metal ions can easily be taken out of the structure and exchanged for other metal ions. Because of the presence of these cations, zeolites are usually used as ion exchangers and catalysts. Its stable framework architecture also makes it an excellent molecular sieve [6].

Zeolite Y has two types of cavities within its structure – the sodalite cavity that measures 5 Å in diameter with access through 2.5 Å windows; and the supercage of 13 Å diameter with access through 7.5 Å windows [7]. Due to the mobility of the Na^+ ions (with a radius of 0.95Å), it is readily replaced by ferrous (Fe^{2+}) ions, which has a radius of 0.8Å [8].

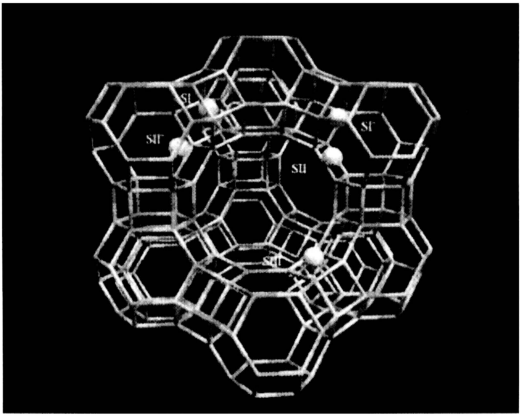

Fig. 2.2: The zeolite Y structure in the dehydrated state. Positions occupied by metal ions within the structure are indicated by the spheres (taken from [5]).

2.2 Iron Oxides

Iron oxide is one of the most common compounds found in nature. There are 6 types of iron oxides, with four of them being polymorphs of Fe_2O_3. Table 2.1 compiles a list of all the iron oxides with some of its important characteristics.

Maghemite is structurally similar to magnetite, possessing a defect spinel structure while its chemical formula is more similar to hematite [9].

Iron oxide is useful in many diverse fields, especially in industrial chemistry technology as pigments, tapes and catalysts. Although its most important application is as ores for the iron and steel industry, it is also used extensively as pigments. In 1989, iron oxides made up 11% of the world pigment production, second only to TiO_2 [10].

Table 2.1: A summary of the iron oxides and their general characteristics

Types of Iron Oxide	Characteristics
Hematite, α-Fe_2O_3	Red (fine), black (coarse). Corundum structure. Extremely stable, the end member of transformations of other oxides.
Magnetite, Fe_3O_4	Black. Ferrimagnetic. Inverse spinel structure.
Maghemite, γ-Fe_2O_3	Red-brown. Ferrimagnetic. Isostructural with magnetite but with cation deficient sites. Product of heating other Fe oxides in presence of organic matter.
β-Fe_2O_3	Rare. Only synthesized in laboratory.
ε-Fe_2O_3	Rare. Only synthesized in laboratory.
Wüstite, FeO	Black. Rock salt structure.

There are only 2 types of magnetically useful iron oxides: magnetite and maghemite. Maghemite is the preferred iron oxide for use as magnetic pigments in electronic recording devices since the late 1940s due to its moderate cost and chemical stability. Fe_2O_3 is also used as the starting material in the production of hard ferrites such as barium ferrite, which are useful in applications such as permanent magnets and high density digital storage media. A relatively new application since it was developed over twenty years ago is the ferrofluid. Raj & Moskowitz [11] reported an ever-increasing usage of ferrofluids since they were first developed. Ferrofluids are liquid magnets containing nanometer-sized magnetic iron oxide particles in aqueous or organic media exhibiting a high degree of colloidal stability in a magnetic field gradient.

2.3 Magnetic Properties

Magnetic nanoparticles exhibit interesting magnetic properties that can be very different from the bulk magnetic properties. All relevant magnetic properties of nanoparticles such as coercivity, blocking temperature, saturation magnetization, and

remanent field are a function of particle size, shape and surface chemistry [12-14]. If the particle size is sufficiently small, ferromagnetic and ferrimagnetic materials will become superparamagnetic. This means that, above a certain temperature, known as the blocking temperature, the material no longer exhibits hysteresis, which is a property of bulk magnetic materials.

The classical theories of superparamagnetism are based on models proposed by Néel and Brown, in which coherent rotation of spins is assumed as the mechanism. Below a critical size, magnetic particles cannot support more than one domain, with magnetic clusters becoming monodomain as opposed to multi-domain in the bulk structure [15-16]. Much of the behavior of single-domain particles can be described by assuming that all the atomic moments are rigidly aligned as a single 'giant' spin. Effectively, this single-domain ferromagnet, loses its ability as an individual magnetic "dot" to store magnetization orientation information when its dimension is below a threshold.

The critical diameter where magnetic particles become single-domain is approximately $2A^{1/2}/M_s$, where A is the exchange constant and M_s is the moment per unit volume [17]. Typical dimensions are in the range of 10-100 nm. A reduction of magnetization values in small ferrite particles is common, but the nature of the spin structure in such particles is not well understood. Spin canting in chemically precipitated maghemite and acicular maghemite recording particles has been demonstrated via Mössbauer spectroscopy. Canting is distinguished from paramagnetism by the presence of a magnetically split Mössbauer spectrum which has incomplete polarization in a large applied field [17].

Magnetite is ferrimagnetic at room temperature, with a Curie temperature (T_C) of 850 K. Its structure has two different cation sites: the tetrahedral sites are occupied by Fe^{3+} and the octahedral sites are occupied by a mixture of Fe^{3+} and Fe^{2+}. These form the

basis for two interpenetrating magnetic sublattices. The preferred direction of magnetization is along the eight [111] cube diagonals. Particles smaller than 6 nm in diameter are paramagnetic at room temperature [18].

Maghemite, like magnetite, is also a ferrimagnet at room temperature. Its T_C has been estimated to be between 820 K and 986 K; the measurement of T_C is difficult because maghemite transforms to hematite above 713 K. Néel proposed the magnetic structure of maghemite consisting of two sublattices that correspond to Fe located on tetrahedral and octahedral sites. Atomic moments within each sublattice are parallel, but those of the two sublattices are antiparallel. Coey and Khalafalla, quoted by Cornell & Schwertmann [19] found that maghemite particles greater than 10 nm in diameter are completely magnetically ordered at room temperature, while smaller particles are superparamagnetic.

The aggregation of ultrafine maghemite particles may also lead to magnetic coupling between particles, i.e. ordering of the magnetic moment, which is termed superferromagnetism. Surface and interfacial effects also influence the magnetic properties of maghemite nanoparticles. Incomplete coordination of atoms at the surface leads to a non-collinear spin configuration, which reduces the magnetization of the small particles. The thickness of this canted layer was estimated by Coey, in the same review by Cornell & Schwertmann [19], to be 1 nm. Finally, Mollard and co-workers, as mentioned by Cornell & Schwertmann [19], found that the specific saturation magnetization decreases linearly with increasing specific surface area, and is also influenced by particle morphology (Batis-Landoulis & Vergnon in [19]).

Hematite, on the other hand, is a paramagnetic material above 956 K (also its T_c). At room temperature, particles below 8 nm in diameter display superparamagnetic relaxation. Otherwise, it is a weak ferromagnet, while at 260 K (the Morin temperature) it undergoes phase transition to become antiferromagnetic. However, the Morin

transition (transformation from ferromagnetic phase to the antiferromagnetic phase) is suppressed for particles below 20 nm in diameter [20].

The energy of a magnetic particle is generally dependent on magnetization direction. At each temperature, there is a critical size below which thermal excitations are sufficient to overcome specific energy barriers and rotate the particle magnetization, thus demagnetizing an assembly of such particles. All this is understood only on a phenomenological level, and the mechanisms by which external thermal excitations and the influence of microstructural details are as yet unknown.

The thermal equilibrium magnetization is described by the Langevin function:

$$L(x) = \coth x - 1/x$$

where $x = M_s VH/k_B T$. M_s is the saturation magnetization, V is the particle volume, H is the applied field, k_B is Boltzmann's constant and T the temperature in Kelvin. This result is identical to the classical treatment of paramagnetism with the atomic moment being replaced by the particle moment, hence the name 'superparamagnetism' was coined. The magnetization at low temperatures is oriented near easy magnetization directions, which correspond to the minima of the magnetic anisotropy energy, separated by energy barriers of certain heights. External fields will change the relative depths of the minima.

As temperature increases, the magnetization will overcome this barrier and turn over to another easy direction with a certain magnetization reversal rate of τ^{-1}. If the magnetization of a collection of particles is measured in a regime where the observation time is comparable to τ^{-1}, then the particles are said to be superparamagnetic [21]. Pfannes et al. [21] suggested that the thermally activated superparamagnetic relaxation of the magnetization of small non-interacting identical particles under the influence on an external magnetic field can be described by a spin-phonon-interaction-like model in

which the total spin of the monodomain particle interacts with strain fields of the crystal.

Frei et al. [16] wrote that below a critical size, a united spin rotation of particles causes magnetization changes. These particles are assumed to be always saturated and possess coercive forces, which depend on various magnetic anisotropies, are calculated to be rather high. These coercive forces were calculated to gradually decrease with respect to particle size when shape anisotropy predominates. They also gave a formula for the critical size:

$$N_b I_s^2 R_c^2/6A = \ln (4R_c/a) - 1,$$

where I_s is the saturation magnetization, R_c is the critical radius of the particle, a: lattice constant, N_b the demagnetizing coefficient along the polar axis, A: the exchange constant (also referred to as stiffness constant, or the Bloch wall coefficient). They also debunked the misconception that the critical size is dependent on crystal anisotropy and elongation.

Fiorani et al. [22] studied the interparticle interactions between nanoparticles in a collective magnetic state. They stated that the problem is an extremely complex one, with complexities of real systems involved, disordered arrangements of particles, volume distributions and the random orientations of easy axes. Jonsson et al. [23] affirm that for non-interacting particles, experimental results of individual particles and assemblies of these particles support the existing Nèel and Brown models. However, for interacting particles, dipole-dipole interactions have been shown to cause collective behavior. Dynamical studies of magnetic particle systems with monodispersive nature indicate a critical slowing down at a finite temperature, implying the existence of a low-temperature phase resembling spin glass.

2.4 Synthesis of Iron Oxide Particles

Synthetic magnetite can be produced in alkaline aqueous systems by precipitation of a mixture of Fe(II) and Fe(III) salt solution, by oxidation of Fe(II) solutions via green rust [$Fe(OH)_2$] and by interaction of Fe(II) with ferrihydrite [24]. Another pathway involves high temperature reduction of Fe(III) oxides (for example, with H_2). Maghemite is formed topotactically by wet or dry oxidation of magnetite or by heating lepidocrocite (γ-FeOOH). Various synthesis pathways of iron oxides are shown in Fig. 2.3, which is taken from Cornell and Schwertmann [24].

Many methods have been utilized to synthesize nanostructured maghemite particles, including sol-gel processing [25-27], Massart's procedure (coprecipitation of Fe(II) and Fe(III) salts in alkaline medium) [28], using hydrazine as a reducing agent of iron salts [29], ball milling of lepidocrocite, γ-FeOOH [30], hydrolysis and pyrolysis of akaganeite (β-FeOOH) and lepidocrocite [31] as well as chemical reaction of mixtures of Fe (II)- and Fe (III)-oxalate salts [32]. Maghemite nanoparticles has been successfully synthesized in a microwave plasma using $FeCl_3$ or $Fe_3(CO)_{12}$ as the precursor [33], through vaporization condensation in a solar furnace [34], by spray pyrolysis [35], using a d.c. current by an electrochemical method [36], by wet chemical processing [37], and also through the use of microemulsions [14, 38].

Means of maghemite particle size controls in the nanometer range include varying the micellar concentration and temperature during the precipitation of ferrous dodecyl sulfate micellar solution with methylamine [39], and using citrate ions to confine the particle dimensions to as small as 2nm [40]. A wire electrical explosion (WEE) method to produce maghemite in a single step has also been successful in producing uniform particles of 4 nm in size [41]. Yaacob et al. [42] also reported using a special aqueous colloidal processing technique of unilamellar vesicles as reactors to produce particles with a mean diameter of 2.6 nm.

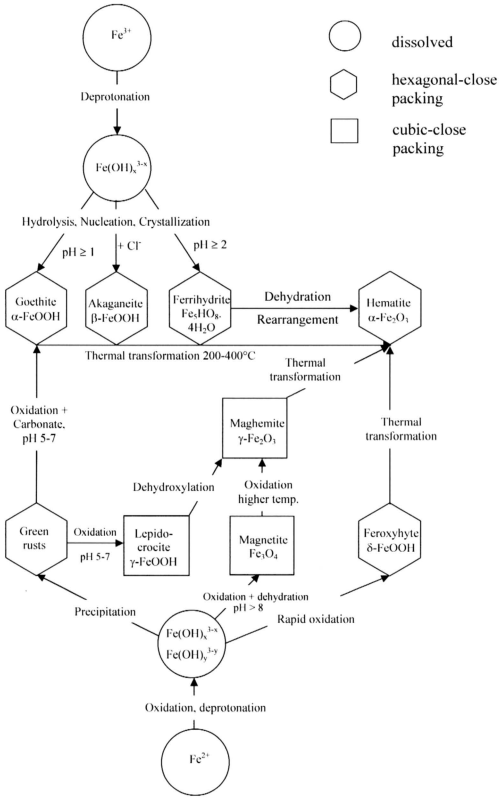

Fig. 2.3: Schematic representation of formation and transformation pathways of common iron oxides (taken from Cornell & Schwertmann [24]).

Maghemite nanoparticles have also been used as one of the powder phases in nanocomposites, such as silica-coated colloidal maghemite particles [43] and Nafion® 117 perfluorinated ion-exchange membranes [44]. It has also been incorporated in an optically transparent magnetic phase [45] as well as a conducting and superparamagnetic film of polyaniline [46]. Maghemite/silica nanocomposites with diverse uses, especially in catalysis have been reported [47-50].

Current applications of magnetic nanoparticles are as the active component of ferrofluids [51-52], in magnetic joints [43], recording tape, flexible disk recording media, as well as biomedical materials and catalysts [17], and reprographic processes [53]. Assemblies of nano-scale magnetic grains make up hard disk recording media, permanent magnets and nanocrystalline soft magnetic materials [17]. Although these diverse technological applications are the focus of much research, magnetic nanoparticles are also used as research tools in areas of materials physics, geology, biology, and medicine [14, 46, 54-56]. More recently, new applications have included electromagnetic interference shielding, electrochromic devices, sensing and actuating technologies, nonlinear optical systems, molecular engineering of nanomotors [46], alcohol sensors in breath analyzers [29], and as gel-based ferrofluid standards for MRI analysis [54].

2.5 Matrix Supported Synthesis

A number of papers in literature have documented the use of a matrix or template to support the synthesis and growth of nanoparticles. Among the matrices reported in use are zeolites, polymer resins and silica materials. The use of a matrix usually includes a process of ion exchange [45-47, 49, 57-62]. These efforts are briefly summarized in the following sub-sections.

2.5.1 Synthesis of Nanoparticles Supported in Zeolite Matrices

The use of zeolites as a constraining matrix is not a new idea. Bogomolov et al. [57], Stramel et al. [58] and Herron et al. [59] are among groups of researchers who have used zeolites as a matrix for obtaining new semiconductor crystals. As early as 1966, studies have been undertaken on introducing iron via organometals such as iron pentacarbonyl [$Fe(CO)_5$], ferrocene ($C_{10}H_{10}Fe$) and covalent compounds like $FeCl_3$ [60] into various types of zeolites. Mulay et al. [60] reported "stuffing" magnetic species within the Linde 13 X zeolite cage structures. They utilized a spray atomizer to produce an iron species-containing aerosol, sprayed onto an agitated 13 X zeolite powder. This method was successful as revealed by the appreciable amount (up to 11.8 wt. %) of Fe (expressed as Fe_2O_3) present in the product. The products were heat-treated in air at 500°C and 900°C to convert the iron phase to Fe_2O_3 and to cause particle growth.

The oxide phase was identified from its XRD spectra. The presence or absence of non-zeolitic material was unable to be detected under electron microscope with magnification up to 15,800. The approximate superposition of magnetic data obtained from the particles produced conformed to the operational definition of superparamagnetism, suggesting the presence of this phenomenon. Magnetic measurement data showed that at a critical size, antiferromagnetic single domains begin to form and the system exhibited minor hysteresis behavior. They obtained a critical radius of ~110 Å for their superparamagnetic system.

The research team led by Garcia [61] investigated the magnetic properties of the ZSM-5 zeolite, which already incorporates iron ions occupying tetrahedral sites (substituting silicon) in its framework. Using the a.c. susceptibility technique, they were able to follow the conversion of in-framework to extra-framework iron atoms. With the knowledge that thermal processing, calcination or hydrothermal treatment will cause the

iron to combine with oxygen forming iron oxide or iron hydroxide aggregates, they observed the existence of a superparamagnetic phase due to small clusters of iron oxide.

In another study, Garcia et al [62] have also reported using zeolites to synthesize constrained magnetic systems. Using the zeolite ETS-10 as support for a novel magnetic system, iron in the form of nitrate salts was introduced into the zeolite by ion-exchange, with heating at 80°C. The Fe ions are ideally incorporated at positions which hosted out-going ions of the same charge. They observed that the effective magnetic moments per iron ion are too small for ferromagnetic particles, suggesting some kind of ferrimagnetic or antiferromagnetic ordering. The magnetic properties of iron-containing ETS-10 zeolites show the coexistence of paramagnetic ions and superparamagnetic clusters.

2.5.2 Synthesis of Nanoparticles Supported in Polymer Matrices

To enhance the processability of nanostructured magnetic particles, as well as to fully realize the various potential applications, they are incorporated with polymers. Ziolo et al. [45] reported isolating a maghemite/polymer nanocomposite that has saturation moments as high as 46 emu/g and is superparamagnetic for lower iron oxide loadings. The particle sizes for the superparamagnetic samples are less than 100 Å. By using a polymer matrix in the form of an ion-exchange resin, they were able to stabilize, isolate and characterize a mesoscopic form of maghemite, unlike most magnetic materials at room temperature, has an appreciable degree of optical transparency in the visible region. Results from optical absorption studies indicate that the small-particle form of maghemite is considerably more transparent to visible light than the single-crystal form. Tang et al. [46] have prepared a maghemite/polyaniline nanocomposite film that has conductance of up to 237 S/cm. The films are also superparamagnetic, with a blocking temperature for the nanocomposite around 63-83 K.

2.5.3 Synthesis of Nanoparticles Supported in Silica Matrices

According to Zhang et al. [49], the use of inorganic matrix such as silica derived from sol-gel is an effective means of tailoring a uniform particle size and controlling the homogenous dispersion of ultrafine clusters of magnetic material. Using the sol-gel method, they produced a maghemite/SiO_2 nanocomposite. Their SiO_2-based gel containing $-SO_3^-$ groups was produced from 3-bromopropyltrimethoxysilane. The bromide groups allow for sulfonation with $NaHSO_3$, and the methoxy groups can undergo hydrolysis and condensation to form an inorganic polymer network at 70°C. Ion-exchange was conducted with a $FeCl_2$ solution whereby the Fe(II) cations are embedded in the gel matrix and converted to $Fe(OH)_2$ clusters by the addition of NaOH and further oxidized to Fe_2O_3 by the action of H_2O_2. The maghemite particles are revealed as elongated crystalline clusters with diameters of 4 nm and lengths of 10-20 nm. Superparamagnetic relaxation and the non-collinear moment of the surface spins in the small particle assembly were used to explain the rapid increase in magnetization as the sample was subjected to a rising magnetic field.

Cannas et al. [47] managed to produce 4-6 nm particles incorporated in silica from mixtures of tetraethylorthosilicate (TEOS) and hydroalchoolic solutions of iron nitrate. The gels were subjected to thermal treatments ranging from 300-1000°C. However, it was difficult to obtain samples where maghemite was the only iron oxide phase present. Hematite, as well as amorphous ferrihydrites, which are the precursors of maghemite, were found in all samples together with maghemite. The zero-field-cooled (ZFC) and field-cooled (FC) susceptibility curves are typical of superparamagnetic materials, with susceptibilities ranging from 0.05 – 0.2 emu/mol. Particle growth was observed with increasing treatment temperature, as seen in TEM photos and supported by the narrowing of peaks in XRD patterns.